REVISTA MATÉRIA V.23 N.02
ISSN 1517-7076 artigo e-12065, 2018

Synthesis and characterization of nanostructured TiO_2 and TiO_2/W thin films deposited by co-sputtering

Leandro García González [1], Luis Zamora Peredo[1], Daniel de Jesús Araujo Pérez[1], Joaquín Villalba Guevara[1], Nelly Flores Ramírez[2], Salomón Ramiro Vásquez García[3], María Guadalupe Garnica Romo [4], Teresa Hernández Quiroz[1], Julián Hernández Torres[1]

[1] Centro de Investigación en Micro y Nanotecnogía - MICRONA – Universidad Veracruzana CP:94294, Boca del Río, Veracruz. México.
e-mail: leagarcía@uv.mx
[2] Facultad de Ingeniería en Tecnología de la Madera – Universidad Michoacana de San Nicolas de Hidalgo, Morelia, Michoacán. México.
[3]Facultad de Ingeniería Química – Universidad Michoacana de San Nicolas de Hidalgo, Morelia, Michoacán. México.
[4] Facultad de Ingeniería Civil – Universidad Michoacana de San Nicolas de Hidalgo, Morelia, Michoacán. México.

ABSTRACT

Nanostructured TiO_2 and TiO_2/W thin films were deposited on Corning glass substrates by RF and DC magnetron co-sputtering at room temperature, using three targets of TiO, Ti and W. After deposition, samples were subjected to an annealing treatment in air at 500 °C for 3 hrs. The effect of the annealing treatment and tungsten addition to the TiO_2 matrix were studied by Raman spectroscopy and X-ray diffraction. Morphology and composition was studied with field emission scanning electron microscopy and optical characterization was made with UV-Vis spectroscopy. All the obtained samples presented an amorphous TiO_2 phase; however, after the annealing treatment, a crystallization process from amorphous to anatase phase occurred with gain sizes between 15.6 and 18.3 nm, additionally, a small amount of rutile was also observable. The SEM images corroborated the XRD behavior, besides it was possible to calculate the thickness of the films which was greater for the W-doped films owing the extra power of the sputtering growth, and after the samples had the thermal treatment the thickness decreased due to a more organized structure. Finally, the UV-vis transmittance analysis revealed that the transmittance is higher in heat-treated films as compared to those without any thermal treatment; also, the TiO_2 thin films showed a greater transmittance than the W doped TiO_2 films, reaching 91%. The lack of transmittance in the non-thermal-treated films made it impossible to compute the band gap of the films; nevertheless, for the thermal-treated films the band gap had a minimal change to the classic TiO_2 bang gap value, even for the W doped sample, providing them with the benefits of the tungsten within the same TiO_2 structure due to a great homogenization on the structure.

Keywords: Sputtering, TiO_2, annealing treatment, Raman, XRD, Photoluminescence, UV-Vis.

1. INTRODUCTION

The titanium dioxide (TiO_2) is one of the most studied materials, owing its exceptional structural, optical, and electronic properties. The TiO_2 is known for its existence in three polymorphic forms: Anatase (tetragonal), rutile (tetragonal) and brookite (orthorhombic), where the tetragonal crystallographic structures, anatase and rutile, are the most used. The rutile phase has a bandgap of 3.10 eV [1,2], with a high refraction index [3,4] and a better chemical and thermal stability. The rutile phase has applications as optical coatings, solar energy converters or protective layers in microelectronics applications. On the other hand, the anatase phase shows a bandgap of 3.23 eV with a relatively low refraction index [5]. The anatase phase is good for applications such as gas sensors applications, solar cells, self-cleaning windows, anti-fog glasses, and photocatalytic applications [6]. Finally, the brookite belongs to a group of minerals called hydrothermal, this means that it is formed by dissolution and precipitation processes related to the magma solidification in fissures on preexistent rocks, in the last decades the interest for these materials has been increasing due to their applications, e.g. as deodorization, protection against atmospheric agents or as residual water treatment; one characteristic of the brookite is that is photo-sensible to any kind of light, in contrast, anatase only reacts with ultraviolet light.

Corresponding Author : Leandro García González Received on: 01/08/2017 Accepted on: 06/09/2017

10.1590/S1517-707620180002.0401

Due to the wide amount of applications on diverse fields, the nanostructured TiO_2 thin films have attracted a lot of interest especially for its effects of quantum confinement. One of the most proliferous applications of the TiO_2 is related to the photocatalytic activity, thereby the TiO_2 could be used as an electrode or multilayer structures in photovoltaic devices that provide a direct electric track for the photo-generated electrons, which lead to a better efficiency of a solar device [7], therefore the TiO_2 is greatly used as a type n semiconductor in such photocatalytic applications [7,8]. Recently, the use of TiO_2 as a transparent conductor oxide material (TCO), has gain a generalized attention because their advantageous electronic properties and the resulting d-electron conductivity, differing from other TCOs materials, like the indium-tin oxide (ITO), that have conductivity of s-electrons. Currently, there are diverse techniques for the production and synthesis of these kind of materials, in bulk or particles like sol-gel [8,9], or in the form of coatings or thin films known as the chemical vapor deposition (CVD) [10,11] and physical vapor deposition (PVD) [13]. Some important CVD methods are the plasma assisted chemical vapor deposition (PECVD) [12] or the metal-organic chemical vapor deposition (MOCVD); On the other hand, PVD include several methods, one of them is the magnetron sputtering [14] in direct current (DC) [15] or radiofrequency (RF) [16] or a combination of both DC and RF known as co-sputtering [15,16].

The titanium and tungsten are elements of good chemical stability, with low cost and a profitable bandgap which limits the photocurrent. The use of tungsten as a dopant agent in TiO_2 is a good option alternative, since it can allow the liberation of up to two electrons per dopant atom. This is a good property that allows the use of low amounts of dopant but maintaining the same effect as a higher amount of other dopant specimens, which also leads to low strengths in the crystalline structure. Additionally, the tungsten is an ideal dopant for the TiO_2 matrix, because it often occurs in the 6+ oxidation state which has a smaller ionic radius than the Ti4+. Therefore, this work focus on the fabrication of TiO_2 thin films with and without W dopant, while trying to control the crystalline phases of the TiO_2 based on the growth parameters of the co-sputtering technique and an annealing treatment. The goal is to produce the films without the use of reactive gases, because most TiO_2 thin films publications study the need of using oxygen during the sputtering process [4,14,17]. Finally, we studied the effect in the change of the structure and optical properties caused by the W inclusion and the annealing temperature to study their performance in applications such as photovoltaic cells, photocatalytic or solar energy converters.

2. MATERIALS AND METHODS

The synthesis of the TiO_2 thin films with and without W doping was performed on Corning glass substrates with dimensions of 75x24x12 mm; the substrate was previously cleaned to obtain a better adherence with the films during the deposition process. The cleaning consisted in four different ultrasonic baths, of 10 min each, inside the ultrasonic cleaner AS5150B; the four baths were the (1) distilled water, (2) soap solution, (3) a 1:1:1 mixture of ethanol, xylene and acetone and (4) a bath in pure ethanol, then the substrates were dried with nitrogen gas and placed in the sputtering vacuum chamber. For the sputtering deposition, an Intercovamex V3 sputtering system was used. A co-sputtering arrangement was used with three targets: In the direct current (DC) source a titanium target was placed, and in radiofrequency sources two targets were placed titanium monoxide (RF1) and tungsten (RF2) for the doped samples. When the vacuum inside the chamber reached a value of $5x10^{-6}$ Torr the working gas was inserted, no oxygen was needed for the synthesis of the samples, only Argon gas flow was used at 15sccm which caused a working pressure of $2x10^{-2}$ Torr, the deposition process lasted 30 min for all samples with and without doping.

After the thin films growth, two films (one with W doping and other without it) received a thermal annealing treatment one at a time. The treatment was done at atmospheric air using 2 steps, the first one at 250°C for 30 min and then a 500°C for 3 hr. After that, the samples where cooled overnight at room temperature. Characterization of the samples was made by different techniques. Microstructure studies were performed with X-ray diffraction using a Bruker D8 Advance diffractometer with a Cu lamp corresponding to a wavelength of 1.642 nm and a swept in 2θ from 20° to 70° with 0.01 step size and 1s step exposure, the equipment was configured for a grazing incidence angle using a Göbel mirror with a 1mm opening and 1° incident angle - θ. The samples were then analyzed with the PDF-2 database from the ICDD. Additionally, Raman Spectroscopy was analyzed with a Thermo scientific DRX Raman. The DRX model uses a laser beam of 532nm, with a spectral range from 50 to $3500cm^{-1}$, the pin hole detector was used with a confocal depth of 1.7µm, and a 10mW potency was used with a 10s collection time. The Morphology and chemical analysis was studied with field emission scanning electron microscopy (FE-SEM) technique in a Jeol JSM-7600F microscope, with a voltage of 15kV in a $9.6x10^{-5}$ Pa vacuum using secondary detectors in GB-LOW mode and using the Jeol special mode, ideal to see “nano” resolution without charging the sample. Addition-

ally, the energy dispersive X-ray spectroscopy was used to do an elemental analysis at 8 mm working distance and six seconds process time. Finally, optical characterization was done with UV-vis spectroscopy using a PerkinElmer Lamdba 365 spectrophotometer, with a wavelength swept from 190 to 700 nm in 300s run time and response time of 0.1s.

3. RESULTS AND DISCUSSION

3.1 Microstructure

The XRD diffractograms are seen in Figure 1, however, only the diffractograms of the samples with annealing treatment are presented since the samples without thermal treatment where completely amorphous. The disordered phases obtained from the samples after the sputtering are not unexpected since controlling the phase by this method is not easy [6,18], but after the thermal treatment the diffractograms changed to form two phases as seen in Figure 1. The anatase phase corresponding to the PDF 01-075-254 card and the rutile phase that corresponds to the PDF 03-065-0191 card. If we observe Figure 1 the anatase phase is more intense in both samples doped and without W. The crystallization of the samples has been previously reported since the temperature increase the diffusion of atoms in the TiO_2 matrix and gives them more thermal stability [5,17]. However, no tungsten diffractogram is visible for the doped sample, its presence needs to be corroborated below with the EDS elemental analysis, however, if tungsten is present in the sample its absence in the diffractogram could be caused by two factors: the small amount of tungsten is no visible by XRD or there is atom substitution inside the TiO_2 matrix instead of small W nucleation crystals, which is better for optical performance, thence, it is more desirable to obtain a well homogenized structure that contains tungsten without forming an extra phase in the structure that could lead to high stresses and recede the good optical properties of the TiO_2 [6,15].

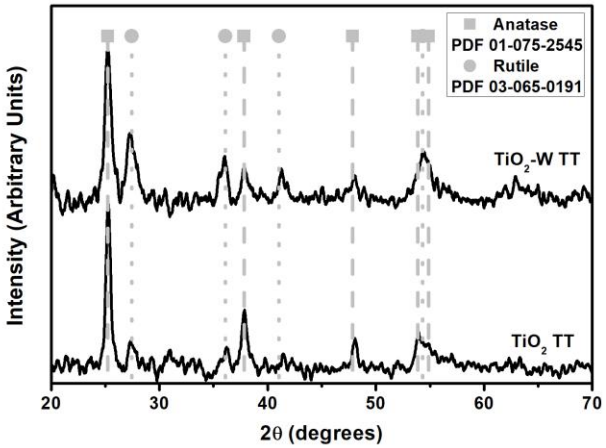

Figure 1: X-ray diffractograms of the samples with thermal annealing treatment.

Additional information obtained from the XRD is in Table 1, where we can observe that the primary phase is Anatase in both samples, however, the addition of tungsten to the TiO_2 matrix favors the formation of rutile phase as the percentage increase to almost 40%. Additionally, the crystal size was computed according to the Scherrer theory and is also reported in Table 1, where the anatase crystal size is 88% bigger than the rutile crystal for the sample without W and 49% bigger for the doped sample. This information is in agreement with the percentage amount of the phases in the sample. The thermal treatment of the films caused a better arrangement to the more stable phase rutile even though the bigger size of the W atom size could cause some stress, the addition of tungsten as a dopant was well received by the TiO_2 network favoring a stable phase formation with relative low treatment temperature [19,20].

Table 1: XRD data extracted from the diffractograms.

Sample	Anatase percentage	Rutile percentage	Anatase Crystal size (nm)	Rutile Crystal size (nm)
TiO_2 TT	86.95	13.05	18.22	9.7
TiO_2-W TT	60.21	39.79	15.64	10.53

The XRD information was corroborated with the Raman Spectroscopy, first in Figure 2.a we can observe the samples with and without doping, without annealing treatment, we can observe that there is not any characteristic band related to the titanium dioxide, which could corroborate the disordered and amorphous nature of the samples. Then in Figure 2.b we can see the Raman spectra for both samples with and without doping with annealing treatment at 500°C, there, a clear change in the spectra is visible. The characteristic anatase at ~145 cm^{-1} band is visible in both samples [21], moreover, a less intense bands at about 400 cm^{-1} and 640 cm^{-1} are observed too, these bands are related to the rutile phase [15] indicating its presence seen in XRD, and the fact that the rutile bands are less intense than the anatase phase corroborates that the samples consist mainly of anatase TiO_2 with small rutile inclusions.

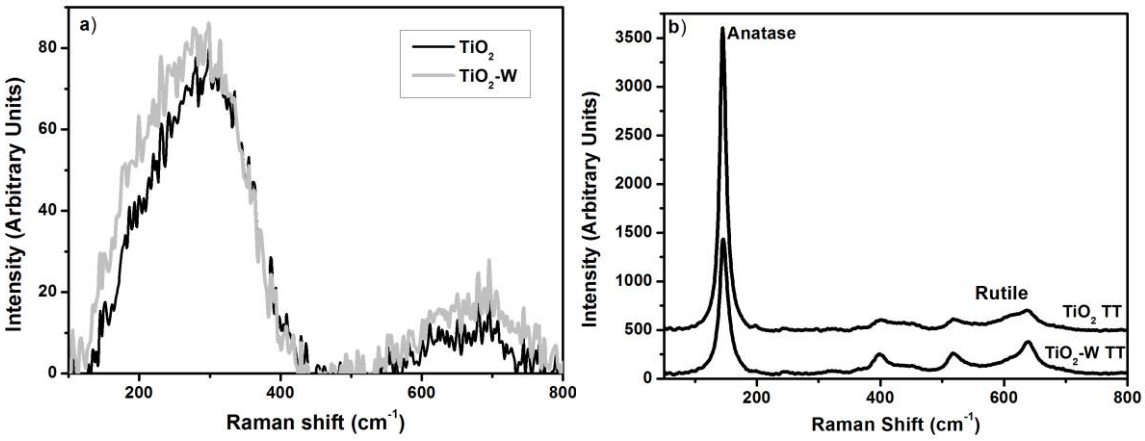

Figure 2: Raman spectra of the TiO_2 samples with and without tungsten doping (a) without annealing treatment and (b) with thermal annealing treatment at 500°C

Again, no band related to the tungsten is seen, probably caused by the small amount of tungsten within the sample or even a great rearrangement of the sample after the W addition, or both. While a small change in the center could be appreciated, the change is barely noticeable and it is not clear whether or not the change is due to the W doping, if the W presence is demonstrated by EDS, this could indicate a great rearrangement of the samples which confers them less atomic stress.

3.2 Morphology and elemental analysis

The FE-SEM studies showed a clear change in the morphology of the samples as seen in Figure 3, both samples without annealing treatment have a disordered surface, with irregular and not-well-formed grains; nevertheless, the grain sizes are very small which could lead to the amorphous structure seen in XRD and Raman spectroscopy, besides, the irregular grain shapes could cause a great amount of different X-ray reflections causing to interfere on each other causing only noise visible in the X-ray diffractograms, moreover, it is possible to distinguish a more irregular surface for the sample doped with tungsten. After the thermal annealing, the grain size increases considerably and the morphology changed. We can see a clear difference between the films with and without tungsten doping with thermal treatment, Figures 3.b and 3.d respectively. The film without tungsten doping show a brighter surface, while the other seems granular and less porous, therefore, the W addition to the film could provide it with more thermal stability [3,21].

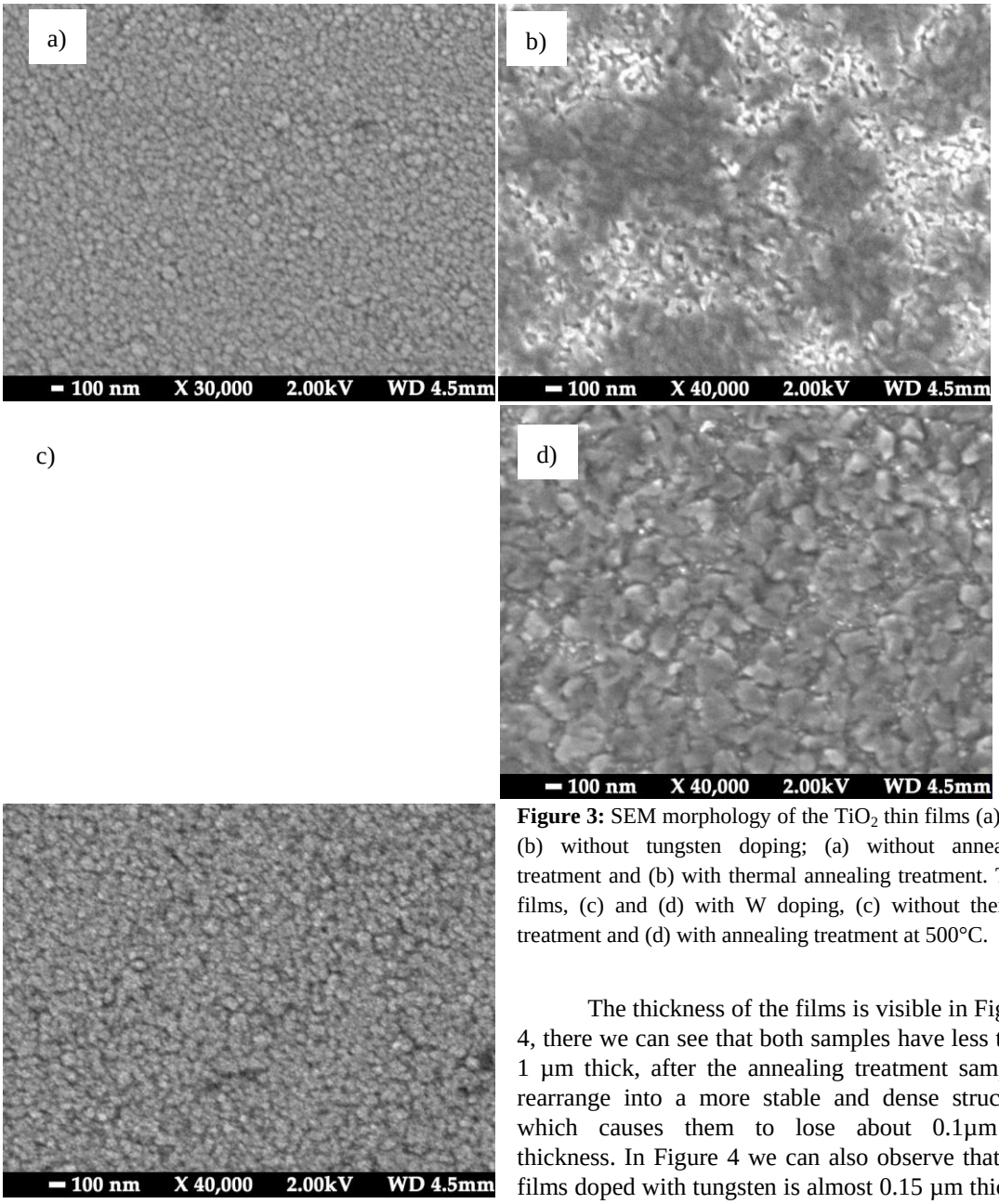

Figure 3: SEM morphology of the TiO_2 thin films (a) and (b) without tungsten doping; (a) without annealing treatment and (b) with thermal annealing treatment. TiO_2 films, (c) and (d) with W doping, (c) without thermal treatment and (d) with annealing treatment at 500°C.

The thickness of the films is visible in Figure 4, there we can see that both samples have less than 1 µm thick, after the annealing treatment samples rearrange into a more stable and dense structure which causes them to lose about 0.1µm of thickness. In Figure 4 we can also observe that the films doped with tungsten is almost 0.15 µm thicker than the ones without doping, this is due the growth conditions during the sputtering process, the extra power of the tungsten RF source increased the deposition rate along with a change of pressure it entails. Besides the thick, we can observe part of the transversal morphology, which is more disordered in comparison to the samples, in agreement with the reported above.

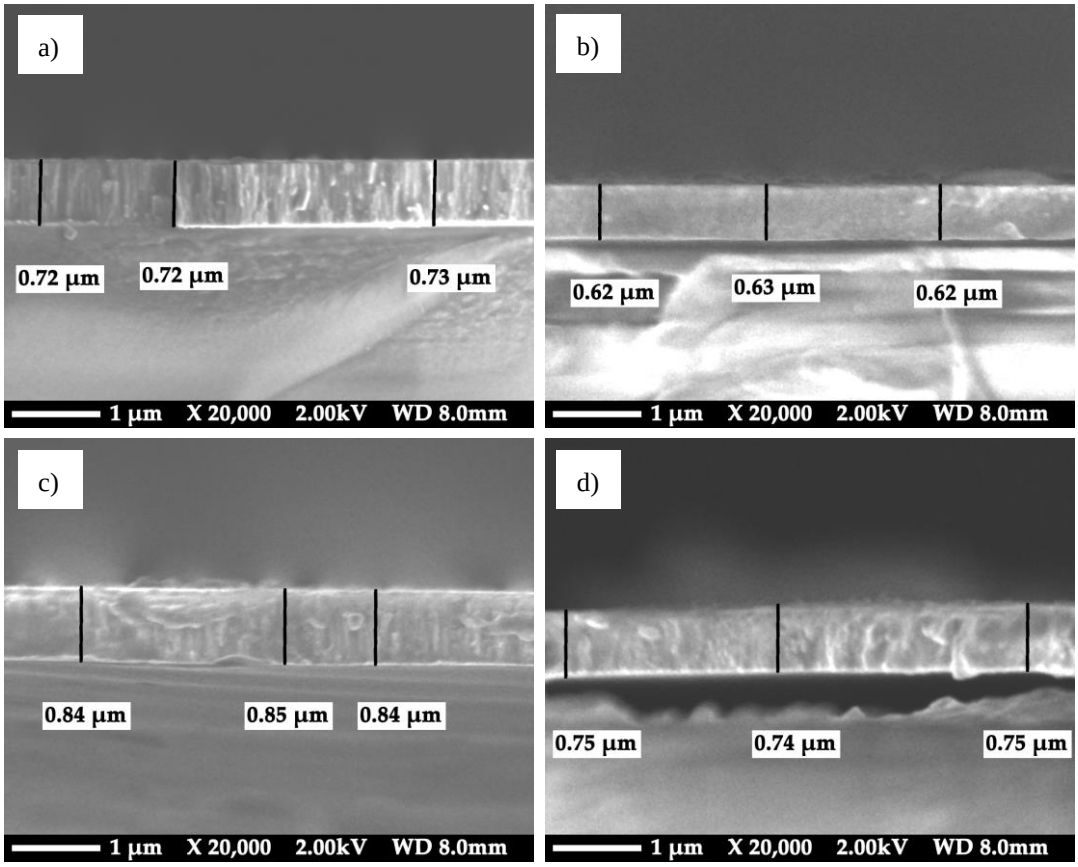

Figure 4: SEM thickness of the TiO_2 thin films (a) and (b) without tungsten doping; (a) without annealing treatment and (b) with thermal annealing treatment. TiO_2 films, (c) and (d) with W doping, (c) without thermal treatment and (d) with annealing treatment at 500°C. µ

Finally, the EDS elemental analysis results are shown in Table 2, we can observe that, as expected, the sample without tungsten doping is completely absent from such element and we can affirm now that the sample with tungsten doping has a small amount of tungsten within, but the amount is only 13% which was no detectable with Raman nor XRD as seen before, this is a good behavior on these films caused by a proper introduction of the tungsten atoms in the network, causing a less stressed primary anatase phase optimal for optical applications. Other behavior that we can see in all samples is that the oxygen is the majoritarian element present in the films, and the amount of oxygen increases as the annealing treatment was done, this could be explained since the treatment was done at atmospheric air so an oxidation process could had happened, this lead to a diminishing in the percentage of titanium and tungsten but the total amount of the elements might remain the same before and after the thermal annealing treatment. It is worth to mention that no silicon is present in the EDS analysis meaning no interference with the corning substrate is seen, this was further corroborated when the samples where repeated on silicon (100) substrate and the oxygen amount remained relatively the same.

Table 2: EDS report data table of the elemental analysis in the films obtained in this work.

Samples	Element composition

TiO_2	O percentage in weight	O Atomic Percentage	Ti percentage in weight	Ti Atomic Percentage	W percentage in weight	W Atomic Percentage
Without TT	46.67	72.38	53.33	27.62	0	0
With TT	53.63	77.59	46.37	22.41	0	0
TiO_2-W						
Without TT	34.56	65.15	51.78	32.61	13.66	2.24
With TT	44.51	73.98	43.81	24.33	11.68	1.69

3.3 Optical behavior

Before we analyze the UV-vis transmittance spectroscopy, it is worth to mention that the samples had a change in its color detectable at simple eye sight, the samples without thermal annealing were pretty opaque with a transmittance percentage near zero whereby they are not presented in this work since they have no optical interest, but after the treatment they became transparent. Therefore, the UV-vis transmittance of the samples with annealing treatment at 500°C have high transmittance values oscillating between 70 and 98% as seen in Figure 5. If we take as reference the 445 nm wavelength, the sample without W doping has a 93.5 % transmittance; while the film doped with W has a lower value of 83.52 %, and we can see that this behavior happens at almost all wavelength window, so we can affirm that the presence of W diminishes the transmittance percentage amount of the TiO_2 film by a small amount. It is worth to mention that these interference oscillations observed in the transmittance spectra show the high optical quality of the samples and they allow the estimation of their thickness [22,23]. Considering a system air/film/substrate, the thickness values of the TiO_2 films with and without doping are about 935 and 860 nm respectively. This result corroborate the behavior seen in SEM images, where the TiO_2 – W is thicker than the TiO_2 sample, but with value deviations of the SEM values between 23 and 37 %, this deviation could be caused since the calculated values were performed using the values of the refraction index reported for TiO_2 and glass substrate. Similarly, the different measurement regions could be another probable cause that it can be attributed to the thickness variations.

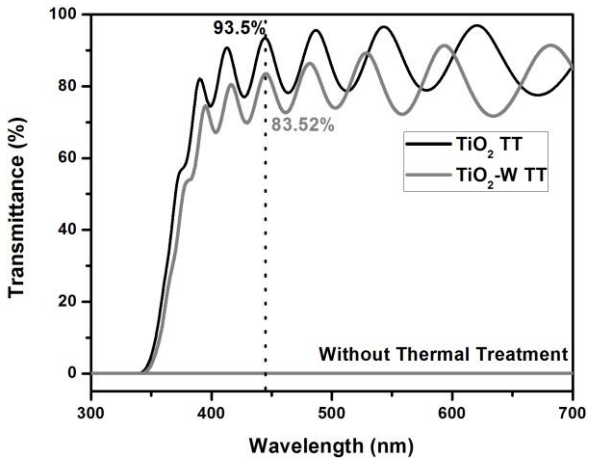

Figure 5: Optical transmittance spectra of the TiO_2 thin films with and without W doping with thermal annealing treatment

In the same way, with the obtained information in the optical transmittance spectra it was possible to compute the bandgap of the samples with annealing treatment using the method reported in [24]. As seen above, the samples without any annealing treatment were opaque so that there is not a significant jump in the adsorption coefficient α. The results are shown in Figure 6.a) for the sample without W doping and 6.b) for the sample with W doping. For the sample without W doping a band gap value of 3.27 eV was obtained and the sample with the doping had a small change to 3.2 eV, if we take as reference the bang gap value of the TiO_2 of 3.21 eV [25]. The band gap values of these films are in agreement with the reported data, even the film doped with W had a similar value because the amount of tungsten is enough to change its transmittance but it was possible to maintain the band gap of the normal TiO_2 since the change was less than 0.1 eV due to a good homogenization of the W inside the TiO_2 network discussed in the XRD data.

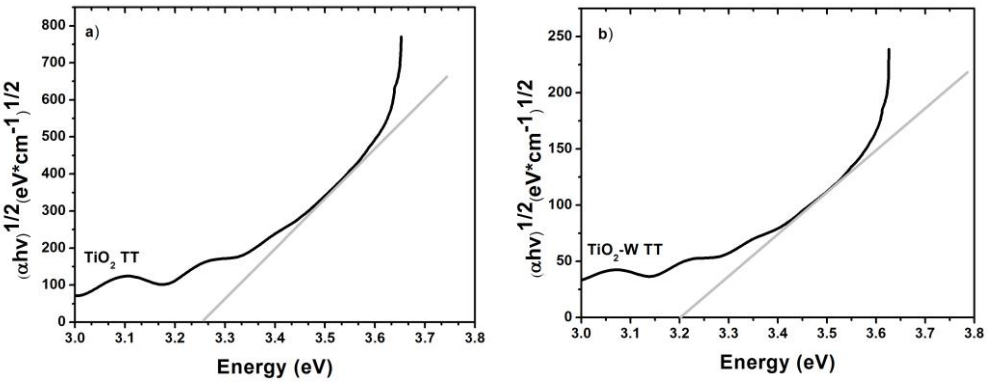

Figure 6: Transmittance optical adsorption to compute the bandgap for the TiO_2 films (a) Without doping and (b) with tungsten doping.

4. CONCLUSIONS

Thin films were deposited on Corning glass as substrate of pure TiO_2 and TiO_2 doped with tungsten, additionally, the samples had a thermal annealing treatment at 500°C. By XRD it was possible to distinguish that the samples are amorphous without thermal treatment no matter if it is doped or not. But after the thermal treatment the films acquire a crystalline structure of mainly anatase and a small amount of rutile; however, the addition of W to the film subserves the formation of rutile up to a 40%. By Raman spectroscopy was possible to corroborate this behavior, but for the sample doped with W it was not possible to distinguish a band nor a diffraction peak that confirms the presence of W, this is mainly because the amount of W in the TiO_2 network is too small as seen by EDS analysis and the thermal treatment favored the homogenization of W in the TiO_2 matrix causing mainly substitutions than interstitials, as it was not possible to distinguish different grain sized nor types by FE-SEM. The optical behavior was studied by UV-vis spectroscopy; we could see that the thermal treatment changed the films to be transparent and the effect of the addition of W in the samples reduces the percentage transmitted while maintaining the band gap near 3.2 eV of the classic anatase TiO_2 even though the rutile phase formation and existence within the sample. The samples without thermal treatment were too opaque and had not enough change in the adsorption coefficient α to determine its bandgap.

5. ACKNOWLEDGMENTS

We would like to thank the PRODEP (before PROMEP) for the support given to the research network: "Materiales Nanoestructurados". We also like to thank to the Universidad Veracruzana for all the support given for the realization, presentation and publishing of this work.

6. BIBLIOGRAPHY

[1] WELTE, A., WALDAUF, C., BRABEC, C., "Application of optical absorbance for the investigation of electronic and structural properties of sol-gel processed TiO2 films", *Thin Solid Films*, v.516, 2008.

[2] GRANQVIST, C.G. "Transparent conductors as solar energy materials: A panoramic review", *Sol. Energy Mater. Sol. Cells*. v.91, pp.1529–1598, 2007.

[3] SATHASIVAM, S., BHACHU, D.S., LU, Y., *et al*., "Tungsten Doped TiO2 with Enhanced Photocatalytic and Optoelectrical Properties via Aerosol Assisted Chemical Vapor Deposition"., *Sci. Rep*., v. 5, 2015.

[4] CHOWDHURY, P., BARSHILIA, H.C., SELVAKUMAR, N., *et al*., "The structural and electrical properties of TiO2 thin films prepared by thermal oxidation", *Phys. B Condens. Matter*. V.403, pp.3718–3723, 2008.

[5] YANG, C., FAN, H., XI, Y., *et al*, "Effects of depositing temperatures on structure and optical properties of TiO2 film deposited by ion beam assisted electron beam evaporation", *Appl. Surf. Sci*., n. 254, pp.2685–2689, 2008.

[6] KARUNAGARAN, B., KIM, K., MANGALARAJ, D., *et al*., "Structural, optical and Raman scattering

studies on DC magnetron sputtered titanium dioxide thin films", *Sol. Energy Mater. Sol. Cells*. v.88 pp.199–208, 2005.

[7] KHAN, A.F., MEHMOOD, M., DURRANI, S.K.., *et al*., "Structural and optoelectronic properties of nanostructured TiO2 thin films with annealing", *Mater. Sci. Semicond. Process*. v.29, pp.161–169, 2014.

[8] FACCHIN, G., CARTURAN, G., CAMPOSTRINI, R., *et al*., "Sol-gel synthesis and characterization of TiO2-anatase powders containing nanometric platinum particles employed as catalysts for 4-nitrophenol photodegradation", *J. Sol-Gel Sci. Technol*., v. 18, pp.29–59, 2000.

[9] YU, J., YU, J.C., HO, W., *et al*., "Effects of alcohol content and calcination temperature on the textural properties of bimodally mesoporous titania", *Appl. Catal. A Gen*., v. 255 pp.309–320, 2003.

[10] BESSERGUENEV, V.G., PEREIRA, R.J.F., MATEUS, M.C., *et al*., "TiO2 thin film synthesis from complex precursors by CVD, its physical and photocatalytic properties*", Int. J. Photoenergy*., v. 5, pp.99–105, 2003.

[11] LEE, H., SONG, M.Y., JURNG, J., *et al.*, "The synthesis and coating process of TiO2 nanoparticles using CVD process", *Powder Technol*., v. 214 , pp.64–68, 2011.

[12] CRISBASAN, A., CHAUMONT, D., SACILOTTI, M., et al., "Study of TiO2 nanomembranes obtained by an induction heated MOCVD reactor", *Appl. Surf. Sci*. v.358 , pp.655–659, 2015.

[13] ABREU, C.S., MATOS, J., CAVALEIRO, A., *et al*., "Tribological characterization of TiO2/Au decorative thin films obtained by PVD magnetron sputtering technology", *Wear*., v.330–331, pp.419–428, 2015.

[14] LIN, Z.A., LU, W.C., WU, C.Y., "Facile fabrication and tuning of TiO2 nanoarchitectured morphology using magnetron sputtering and its applications to photocatalysis", *Ceram. Int.*,v.40, pp.15523–15529, 2014.

[15] WANG, H., LI, Y., BA, X., *et al*., "TiO2 thin films with rutile phase prepared by DC magnetron co-sputtering at room temperature: Effect of Cu incorporation", *Appl. Surf. Sci*., v. 345, pp.49–56, 2015.

[16] WAN, G., WANG, S., ZHANG, X., *et al*., "Transparent conductive Nb-doped TiO2 films deposited by RF magnetron co-sputtering", *Appl. Surf. Sci*. v.357, pp. 622–625, 2015.

[17] KACZMAREK, D., DOMARADZKI, J., WOJCIESZAK, D., *et al*., Hardness of Nanocrystalline TiO2 Thin Films, *J. NANO Res*., .18–19 , pp.195–200, 2012.

[18] MITTERER, C. "PVD and CVD Hard Coatings", In: Compr. Hard Mater., pp. 449–467, 2014.

[19] CHATURVEDI, A., JOSHI, M.P., MONDAL, P, *et al*., "Growth of anatase and rutile phase TiO2 nanoparticles using pulsed laser ablation in liquid: Influence of surfactant addition and ablation time variation", *Appl. Surf. Sci*., 2016.

[20] SELMAN, A.M., HUSHAM, M. "Calcination induced phase transformation of TiO2 nanostructures and fabricated a Schottky diode as humidity sensor based on rutile phase", *Sens. Bio-Sensing Res*., v.11 , pp.8–13, 2016.

[21] ZHOU, M., ROUALDÈS, S., ZHAO, J., *et al*., Nanocrystalline TiO2 thin film prepared by low-temperature plasma-enhanced chemical vapor deposition for photocatalytic applications, *Thin Solid Films*., v.589, pp.770–777, 2015.

[22] GOODMAN, A.M. "Optical interference method for the approximate determination of refractive index and thickness of a transparent layer"., *Appl. Opt.* , v.17, pp.2779–2787, 1978.

[23] HEAVENS, O.S. *Optical properties of thin solid films*, Dover Publications, 1991.

[24] SREEMANY, M., SEN, S. "A simple spectrophotometric method for determination of the optical constants and band gap energy of multiple layer TiO2 thin films", *Mater. Chem. Phys*., v.83, pp.169–177, 2004.

[25] ALAMGIR, W. KHAN, S., *et al*., "Structural phase analysis, band gap tuning and fluorescence properties of Co doped TiO2 nanoparticles", *Opt. Mater. (Amst*). v.38, pp.278–285, 2014.